Обзор ArXiv/astro-ph, 11-15 декабря 2017 года

От Сильченко О.К.

Astro-ph: 1712.03020 (Nature)

Galaxy growth in a massive halo in the first billion years of cosmic history

D. P. Marrone[1], J. S. Spilker[1], C. C. Hayward[2,3], J. D. Vieira[4], M. Aravena[5], M. L. N. Ashby[3], M. B. Bayliss[6], M. Béthermin[7], M. Brodwin[8], M. S. Bothwell[9,10], J. E. Carlstrom[11,12,13,14], S. C. Chapman[15], Chian-Chou Chen[16], T. M. Crawford[11,14], D. J. M. Cunningham[15,17], C. De Breuck[16], C. D. Fassnacht[18], A. H. Gonzalez[19], T. R. Greve[20], Y. D. Hezaveh[21,28], K. Lacaille[22], K. C. Litke[1], S. Lower[4], J. Ma[19], M. Malkan[23], T. B. Miller[15], W. R. Morningstar[21], E. J. Murphy[24], D. Narayanan[19], K. A. Phadke[4], K. M. Rotermund[15], J. Sreevani[4], B. Stalder[25], A. A. Stark[3], M. L. Strandet[26,27], M. Tang[1], & A. Weiß[26]

Сначала на телескопе в Антарктике нашли субмиллиметровый источник

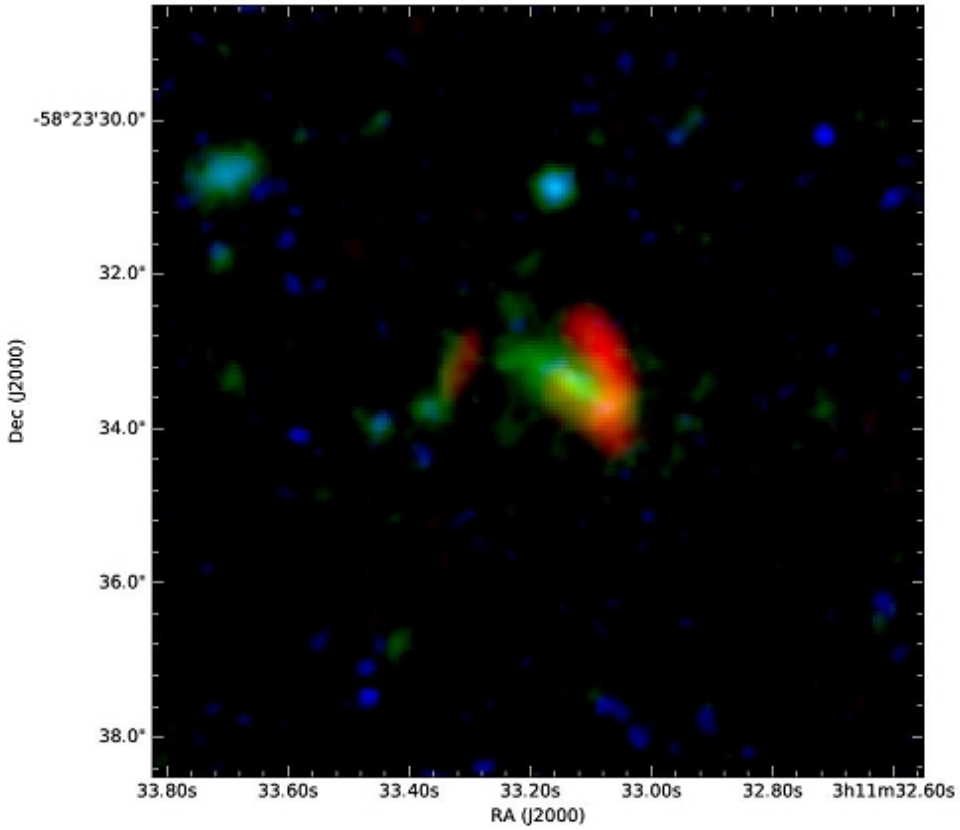

Extended Data Figure 3 | Optical, Infrared, and Millimeter image of SPT0311–58. The field around SPT0311–58 as seen with ALMA and *HST* at 1.3 mm (ALMA band 6; red), 1300 nm (combined *Hubble*/WFC3 F125W and F160W filters; green), and 700 nm (combined *Hubble*/ACS F606W and F775W filters; blue). For emission from $z = 6.9$, no emission should be visible in the ACS filters due to the opacity of the neutral intergalactic medium, while the other filters correspond to rest-frame 160 nm and 160 μm.

Потом закартировали в линиях CO, [CII]158, [OIII]88 мкм на ALMA

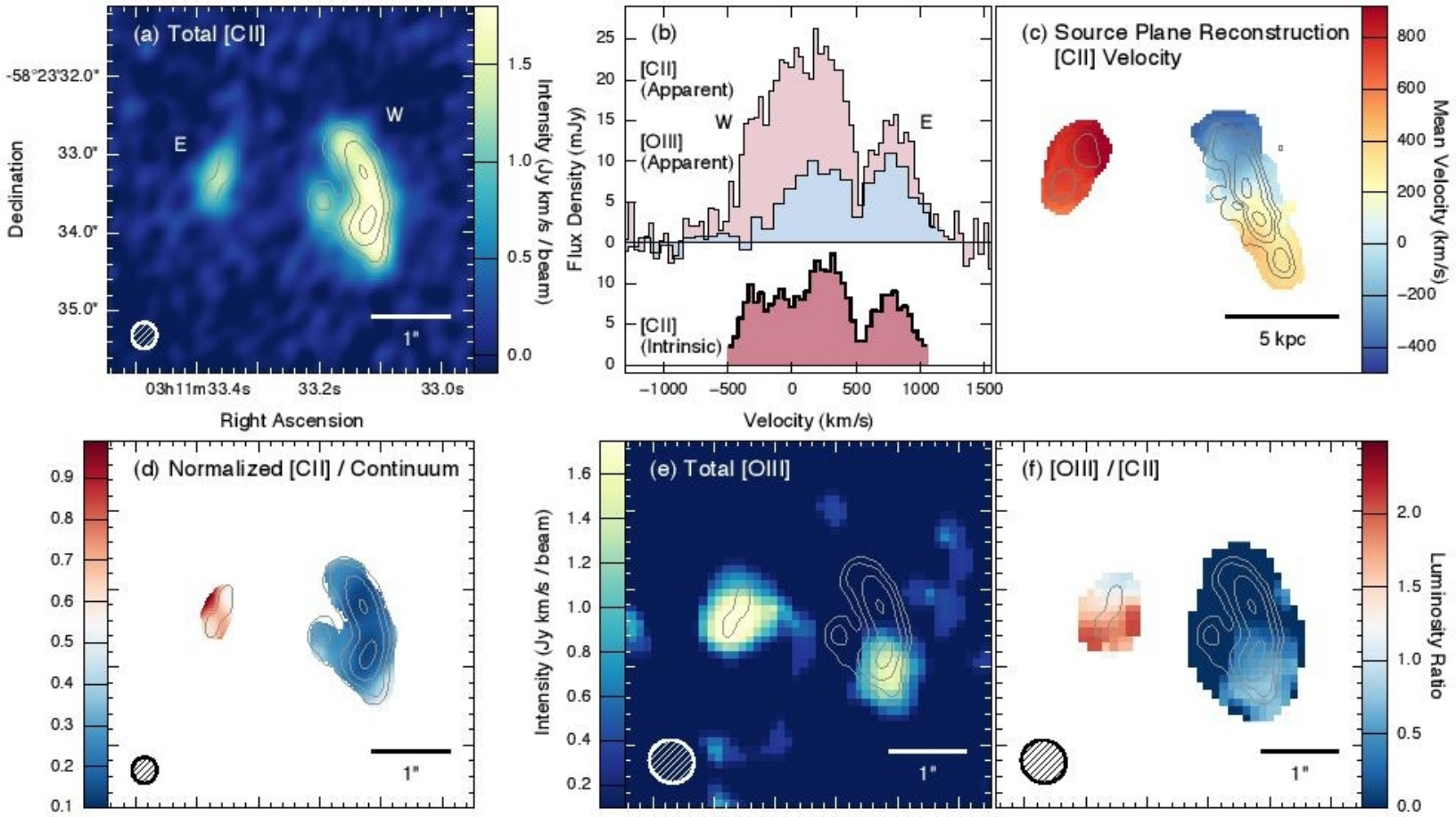

Figure 1 | Continuum, [C II], and [O III] emission from SPT0311–58 and the inferred source-plane

Газа (и пыли) ОЧЕНЬ много!

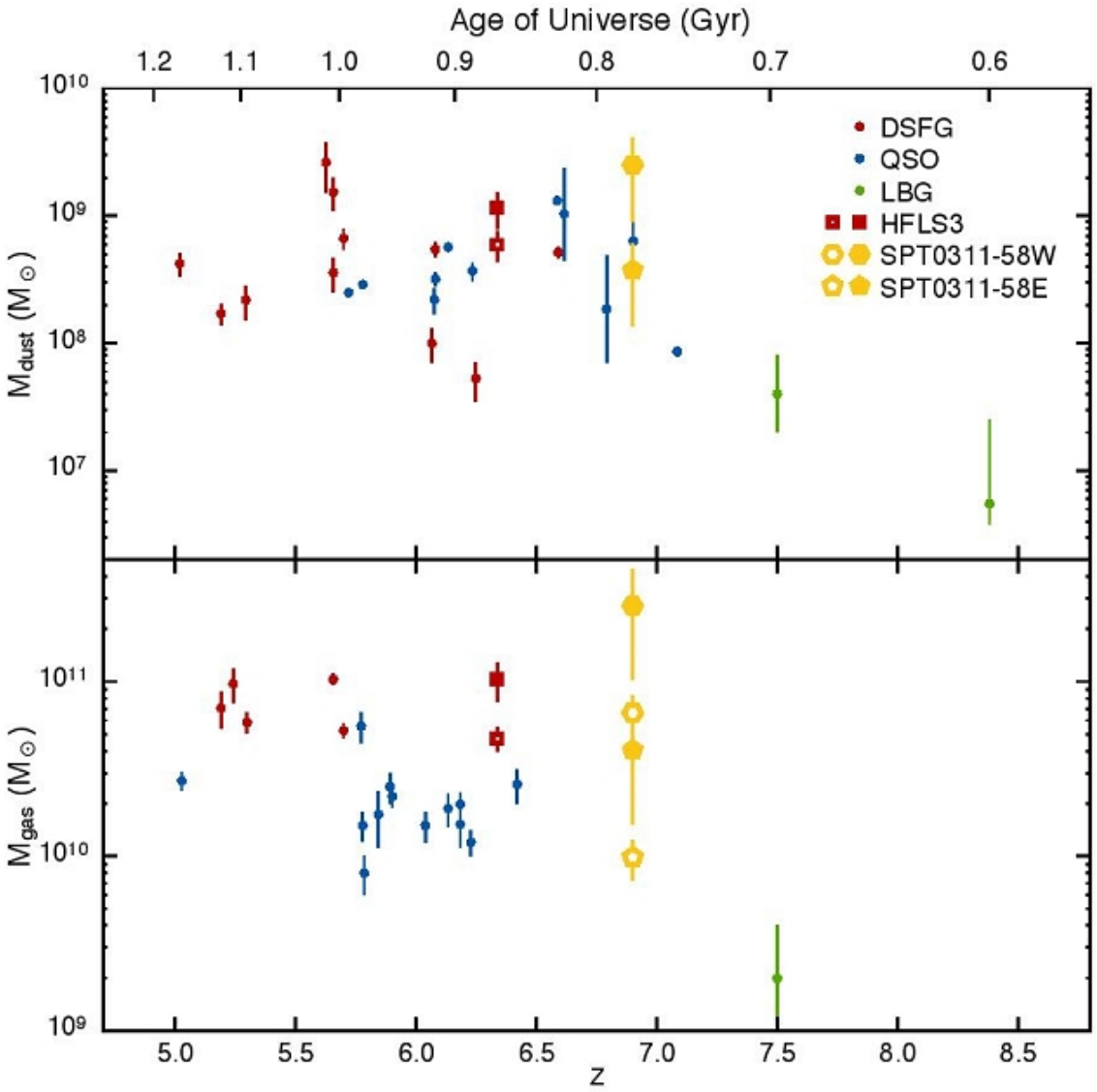

И это должно напрягать космологов

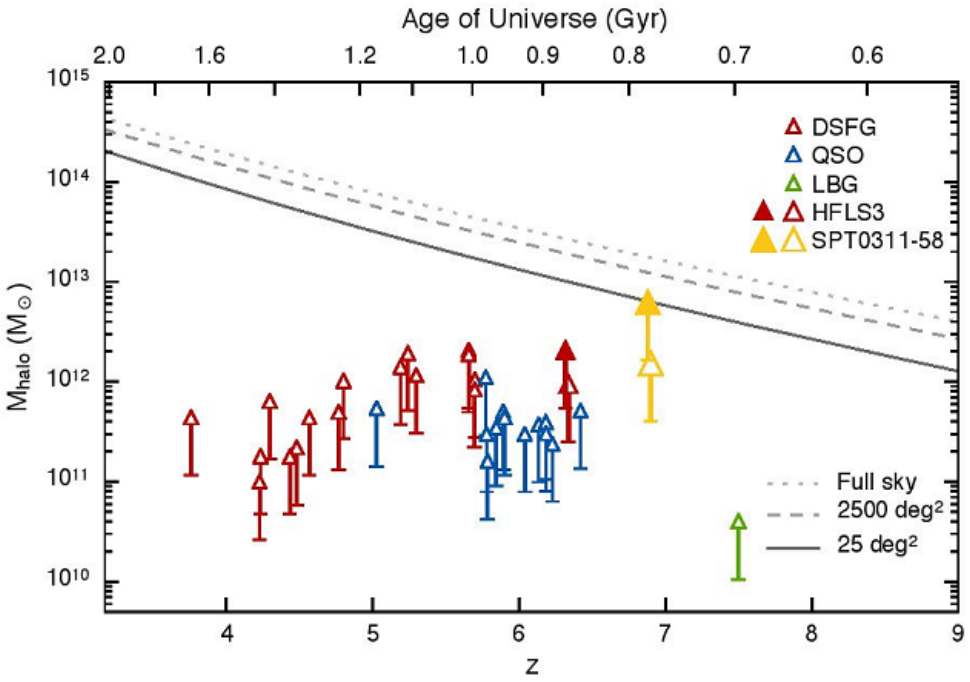

Figure 3 | Halo masses for rare, high-redshift massive galaxies. The dark matter halo mass ($M_{\rm halo}$; defined at an overdensity of 200 times the mean matter density of the universe) is inferred for galaxies in the first 2 Gyr after the Big Bang (see Methods). These masses present a range of lower limits, from the most conservative assumption (lower bars) that all baryons in the initial halo have been accounted for in the molecular gas mass, to the observationally motivated assumption (upper triangles) that the baryonic mass ($M_{\rm b}$) in gas is a fixed ratio of the halo mass $M_{\rm b}/M_{\rm halo} = 0.05$, calibrated through a comparison[3] of simulations and observations spanning $z = 0 - 8$. The most massive halos that are expected to be observable[28] within the whole sky (dotted line), the 2500 deg^2 area of the SPT survey (dashed line), and within the subset of that area that is magnified by a factor of two or more (solid line) are also plotted as

Astro-ph: 1712.03591

The EDGE-CALIFA survey: the influence of galactic rotation on the molecular depletion time across the Hubble sequence

D. Colombo[1⋆], V. Kalinova[1], D. Utomo[2,3], E. Rosolowsky[4], A. D. Bolatto[5], R. C. Levy[5], T. Wong[6], S. F. Sanchez[7], A. K. Leroy[3], E. Ostriker[8], L. Blitz[2], S. Vogel[5], D. Mast[9], R. García-Benito[10], B. Husemann[11], H. Dannerbauer[12,13], L. Ellmeier[14], Y. Cao[6].

[1] *Max Planck Institute for Radioastronomy, Auf dem Hügel 69, D-53121, Bonn, Germany*
[2] *Department of Astronomy, University of California, Berkeley, CA 94720, USA*
[3] *Department of Astronomy, The Ohio State University, 140 West 18th Avenue, Columbus, OH 43210, USA*
[4] *Department of Physics, University of Alberta, 4-181 CCIS, Edmonton, AB T6G 2E1, Canada*
[5] *Department of Astronomy, University of Maryland, College Park, MD 20742, USA*
[6] *Department of Astronomy, University of Illinois, Urbana, IL 61801, USA*
[7] *Instituto de Astronomiá, Universidad Nacional Autonóma de Mexico, A.P. 70-264, 04510 México, D.F., Mexico*
[8] *Department of Astrophysical Sciences, Princeton University, Princeton, NJ 08544, USA*
[9] *Observatorio Astronómico de Córdoba, Laprida 854, Observatorio, X5000BGR Córdoba, Argentina*
[10] *Instituto de Astrofísica de Andalucía (CSIC), Glorieta de la Astronomía s/n, Aptdo. 3004, 18080 Granada, Spain*
[11] *Max-Planck-Institut für Astronomie, Königstuhl 17, D-69117 Heidelberg, Germany*
[12] *Instituto de Astrofísica de Canarias, E-38205 La Laguna, Tenerife, Spain*
[13] *Universidad de La Laguna, Dpto. Astrofísica, E-38206 La Laguna, Tenerife, Spain*
[14] *Department of Astrophysics, University of Vienna, Türkenschanzstrasse 17, 1180, Vienna, Austria*

Выборка: типы от E (NGC5485!) до недопредставленных Sd

2.3 Sample selection

The sample considered in this paper consists of 83 objects, which is the overlap between 126 galaxies from the full EDGE D+E sample and the 238 CALIFA galaxies that have the circular velocity curve modeled by Kalinova et al. (2017a). In most of the analysis, we only use galaxies with inclination below 65°. We explore the effect of inclinations in highly inclined galaxies in Appendix D. There are 71 EDGE galaxies with inclination below this 65° limit, which, when restricted to the samples with dynamical models and that encompass at least one line-of-sight with SNR>2 (for both $\Sigma_{\rm SFR}$ and $\Sigma_{\rm mol}$) results in 39 objects. Fig. 1 shows the comparison between the parent EDGE sample (after inclination cut) and the sample used in this paper. Although there is a significant reduction in the number of galaxies, our sample is still a representation of the EDGE sample (after inclination cut) in terms of the Hubble type, stellar masses, star formation rates, and molecular gas masses. However, very late-type galaxies (Sd) are underrepresented in our sample. Galaxies with $\log(\mathrm{SFR/M_\odot\ yr^{-1}}) > 1$ and $\log(M_{\rm mol}/\mathrm{M_\odot}) > 10$ are also underrepresented with respect to the EDGE sample (after inclination cut).

Цель работы:

- Проверялся «альтернативный закон звездообразования» - Эльмегрина-Силка:

$\forall\ \Sigma(SFR) = \varepsilon\ \Sigma(gas) / \tau(orb)$

- Отсюда прямая пропорциональность между орбитальным периодом и временем исчерпания газа.

Эффективность 5% с большим разбросом

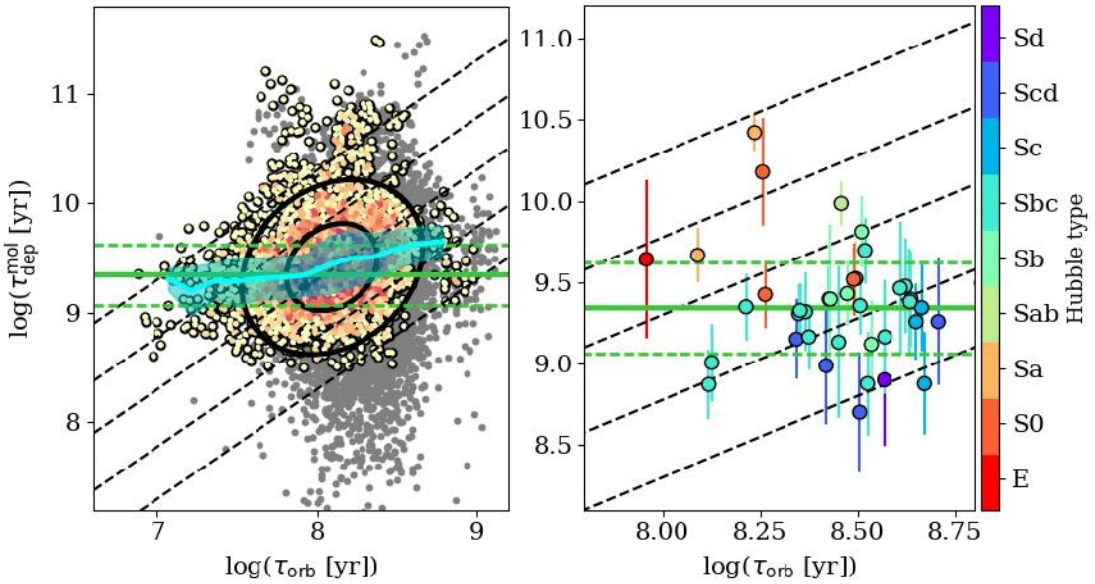

Figure 2. *Left*: The resolved relationship between τ_{dep}^{mol} and τ_{orb} in our EDGE-CALIFA sample. This figure shows that the detected lines-of-sights cluster around the 5% orbital efficiency with a large scatter of 0.5 dex. Coloured circles in the diagrams refer to the detections only, with darker colours represent higher number densities of pixels. The upper and lower limits of τ_{dep}^{mol} are indicated as gray points. Black ellipses mark the 1σ (inner) and 2σ (outer) confidence interval of the data, derived from the Principal Component Analysis (see text). The cyan line and its band indicate the median and interquartile range of τ_{dep}^{mol} within bins of 0.2 dex in τ_{orb}. *Right*: The integrated measurements of the molecular depletion times (calculated within 2 R_{eff}) and the orbital times (measured at 2 R_{eff}). The measurements of τ_{dep}^{mol} and τ_{orb} in Sb-Sbc galaxies (which dominate our sample) are moderately correlated (Spearman rank ~ 0.7) and show

Еще куча корреляция (?) – везде выпадают эллиптические галактики

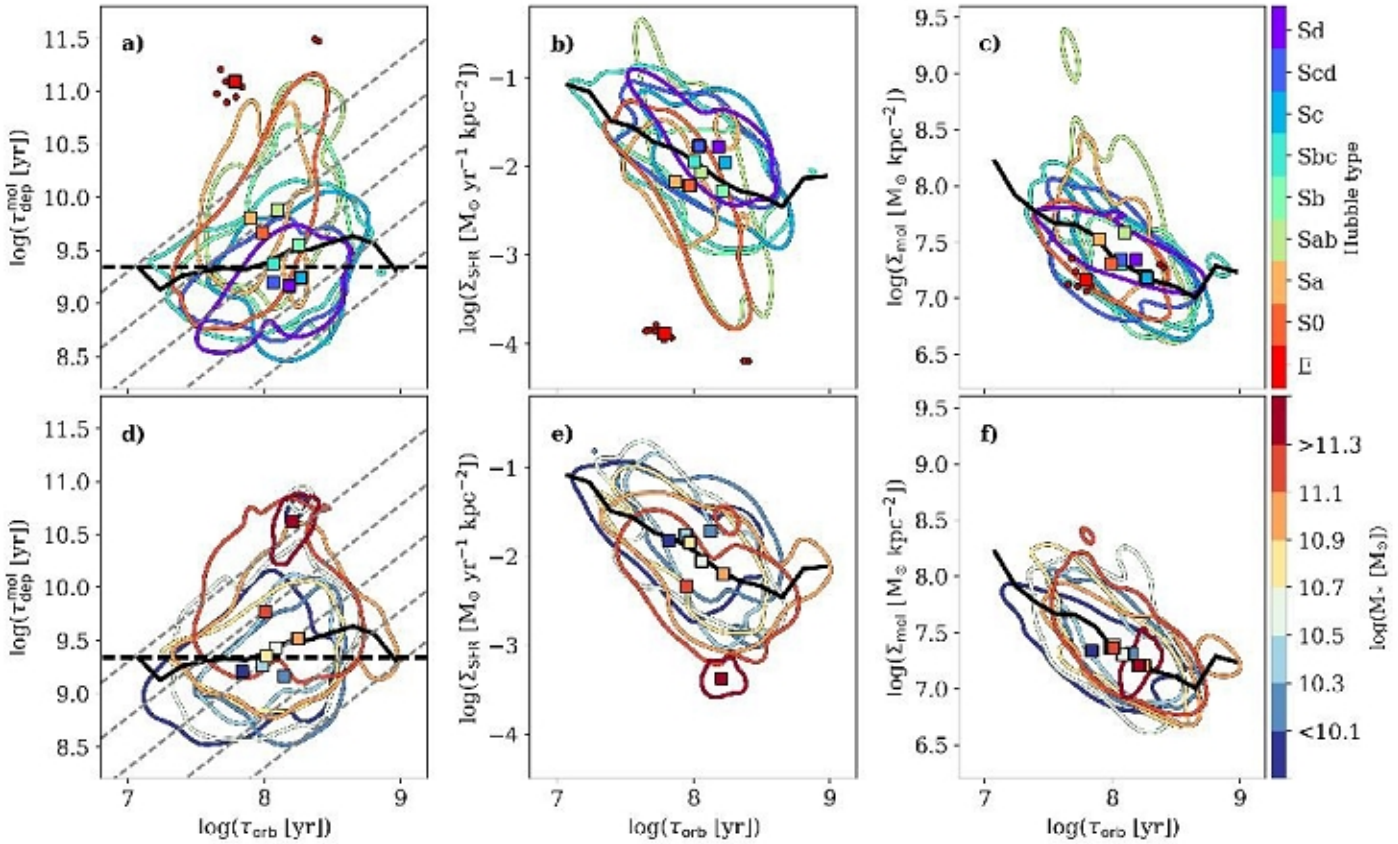

Figure 3. Pixel-by-pixel relations between $\tau_{\rm dep}^{\rm mol}$ (first column), $\Sigma_{\rm SFR}$ (second column), and $\Sigma_{\rm mol}$ (third column) with respect to $\tau_{\rm orb}$, where both $\Sigma_{\rm SFR}$ and $\Sigma_{\rm mol}$ are detected with line-of-sights SNR$>$ 2. The data are color-encoded by Hubble type (first row) and integrated stellar mass (second row). The colored contours indicate the Kernel Density Estimation (KDE)-smoothed surface that contains 95% of the points in a given category. Elliptical galaxies, for which we possess only few line-of-sights, are plotted with red circles, instead of a contour. Colored squares indicate the positions of the quantity medians for each category. The black solid lines indicate the medians of the related quantities within 0.2 dex bins of orbital times. The black horizontal dashed lines in panels *a* and *d* mark the nearby star forming galaxy depletion time of 2.2 Gyr (Leroy et al. 2013), while the gray diagonal lines are the constant orbital efficiencies (from left to right) of 0.5%, 1.7%, 5%, 17%, and 50%. This figure shows that the $\tau_{\rm dep}^{\rm mol}-\tau_{\rm orb}$ and $\Sigma_{\rm SFR}-\tau_{\rm orb}$ relations (panels *a* and *b*) are segregated by the Hubble types, in the sense that the slopes of the relation are shallower from early to late-type galaxies. However, these trends can not be simply attributed to the different stellar masses of galaxies (panels *d* and *e*) nor the molecular gas surface density (panels *c* and *f*).

И этот «морфологический quenching» связан с динамикой, а не с количеством молекулярного газа

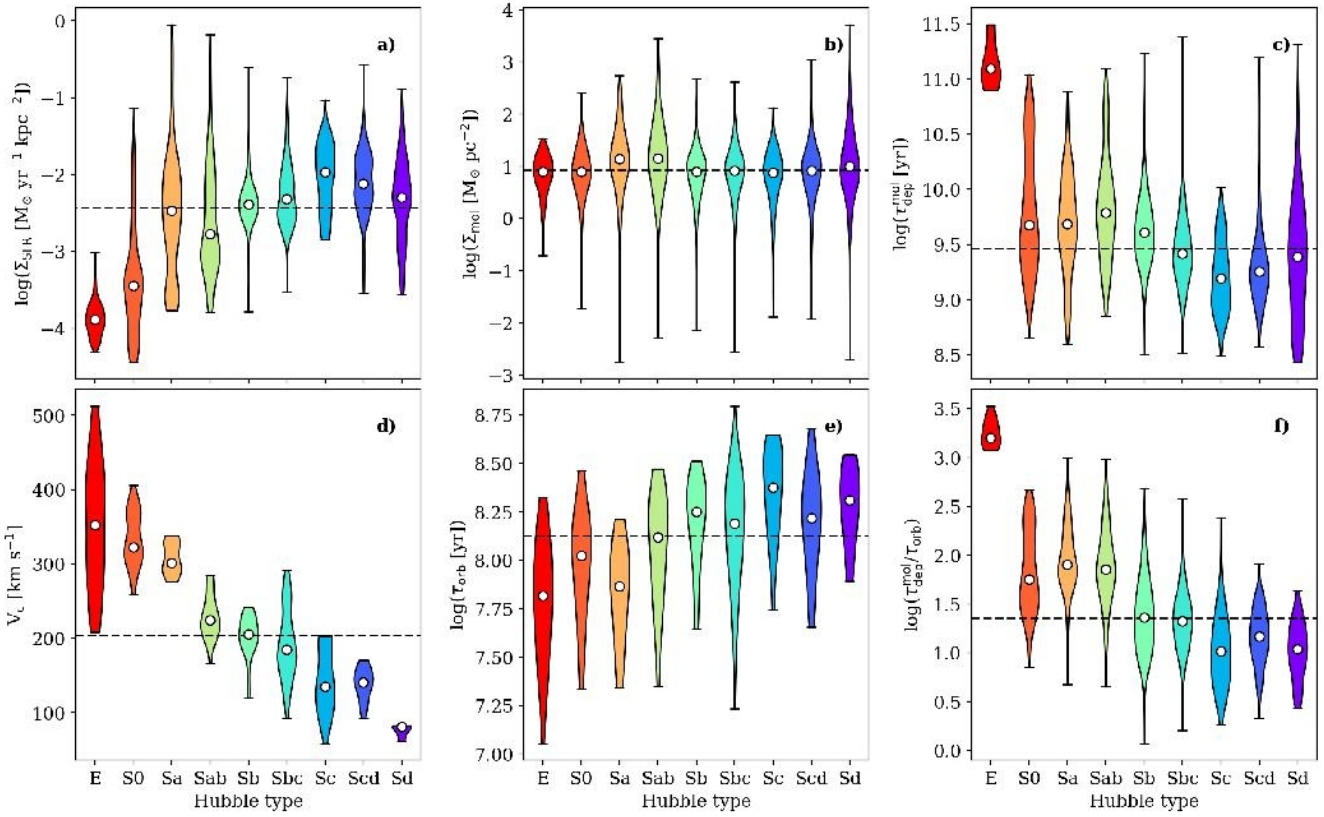

Figure 5. Violin plot representations of the resolved quantities that are studied in this paper across the Hubble types. Violin plots are histograms, where the width along the x-axis indicates the normalized fraction of data at the corresponding y-axis value. The values of $\Sigma_{\rm SFR}$, $\Sigma_{\rm mol}$, $\tau_{\rm dep}^{\rm mol}$, and $\tau_{\rm dep}^{\rm mol}/\tau_{\rm orb}$ are analyzed pixel-by-pixel, while V_c and $\tau_{\rm orb}$ azimuthal averages are calculated within 2 $R_{\rm eff}$. Choosing V_c and $\tau_{\rm orb}$ within 1 $R_{\rm eff}$ renders the trend with Hubble type of the two quantities even more prominent. White circles represent the median values for each Hubble type. Dashed lines show the global median of the

Astro-ph: 1712.04953

Abundance ratios in dwarf elliptical galaxies

Ş. Şen[1,2⋆], R. F. Peletier[1], A. Boselli[3], M. den Brok[4], J. Falcón-Barroso[5,6], G. Hensler[7], J. Janz[8,9,16], E. Laurikainen[9], T. Lisker[10], J. J. Mentz[1,11], S. Paudel[12], H. Salo[9], A. Sybilska[13], E. Toloba[14], G. van de Ven[15], A. Vazdekis[5,6] and C. Yesilyaprak[2]

[1] *Kapteyn Astronomical Institute, University of Groningen, P. O. Box 800, 9700 AV Groningen, Netherlands*
[2] *Dept. of Astronomy and Astrophysics, Faculty of Science, Atatürk University, 25030, Erzurum, Turkey*
[3] *Aix Marseille Université, CNRS, LAM (Laboratoire d'Astrophysique de Marseille), UMR 7326, 13388 Marseille, France*
[4] *Institute for Astronomy, ETH Zurich, Wolfgang-Pauli-Strasse 27, 8093 Zurich, Switzerland*
[5] *Instituto de Astrofísica de Canarias,Calle Vía Láctea s/n, E-38200 La Laguna, Tenerife, Spain*
[6] *Departamento de Astrofísica, Universidad de La Laguna, E-38205 La Laguna, Tenerife, Spain*
[7] *Department of Astrophysics, University of Vienna, Türkenschanzstrasse 17, 1180 Vienna, Austria*
[8] *Centre for Astrophysics and Supercomputing, Swinburne University, Hawthorn, VIC 3122, Australia*
[9] *Astronomy Research Unit, University of Oulu, FI-90014, Finland*
[10] *Astronomisches Rechen-Institut, Zentrum für Astronomie der Universität Heidelberg, Mönchhofstraße 12-14,69120 Heidelberg, Germany*
[11] *Center for Space Research, North-west University, Potchefstroom 2520, South Africa*
[12] *Department of Astronomy & Center for Galaxy Evolution Research, Yonsei University, Seoul 03722, Republic of Korea*
[13] *European Southern Observatory, Karl-Schwarzschild-Strasse 2, 85748 Garching bei München, Germany*
[14] *University of the Pacific, Department of Physics, 3601 Pacific Avenue, Stockton, CA 95211, USA*
[15] *Max-Planck-Institut für Astronomie, Königsstuhl 17, 69117 Heidelberg, Germany*
[16] *Finnish Centre of Astronomy with ESO (FINCA), University of Turku, Väisäläntie 20, 21500 Piikkiö, Finland*

Разнородные наблюдения!

- 26 галактик на 4.2-метровом WHT, двухрукавный спектрограф ISIS, диапазон 4200-5000 A и 5500-6700 A;
- 10 галактик на 2.5-метровом INT, IDS спектрограф с диапазоном 4600-5600 A;
- 3 галактики на FORS2/VLT, 4500-5600 A
- ЛИКСКИЕ ИНДЕКСЫ в модификации Vazdekis.

И хотят соотношения элементов!

Table 2. A summary of the indices used

Telescope	WHT	INT and VLT
Age indicator	$H\gamma_{\rm F}$	$H\beta$
Metal indicator	Fe4383, Fe4531	Fe4531, Fe5270, Fe5335
	Fe5709	Fe 5406, Fe5709, Mgb
Na abundances	NaD	. . .
Ca abundances	Ca4227	. . .
Mg abundance	. . .	Mgb

Магний и железо еще туда-сюда…

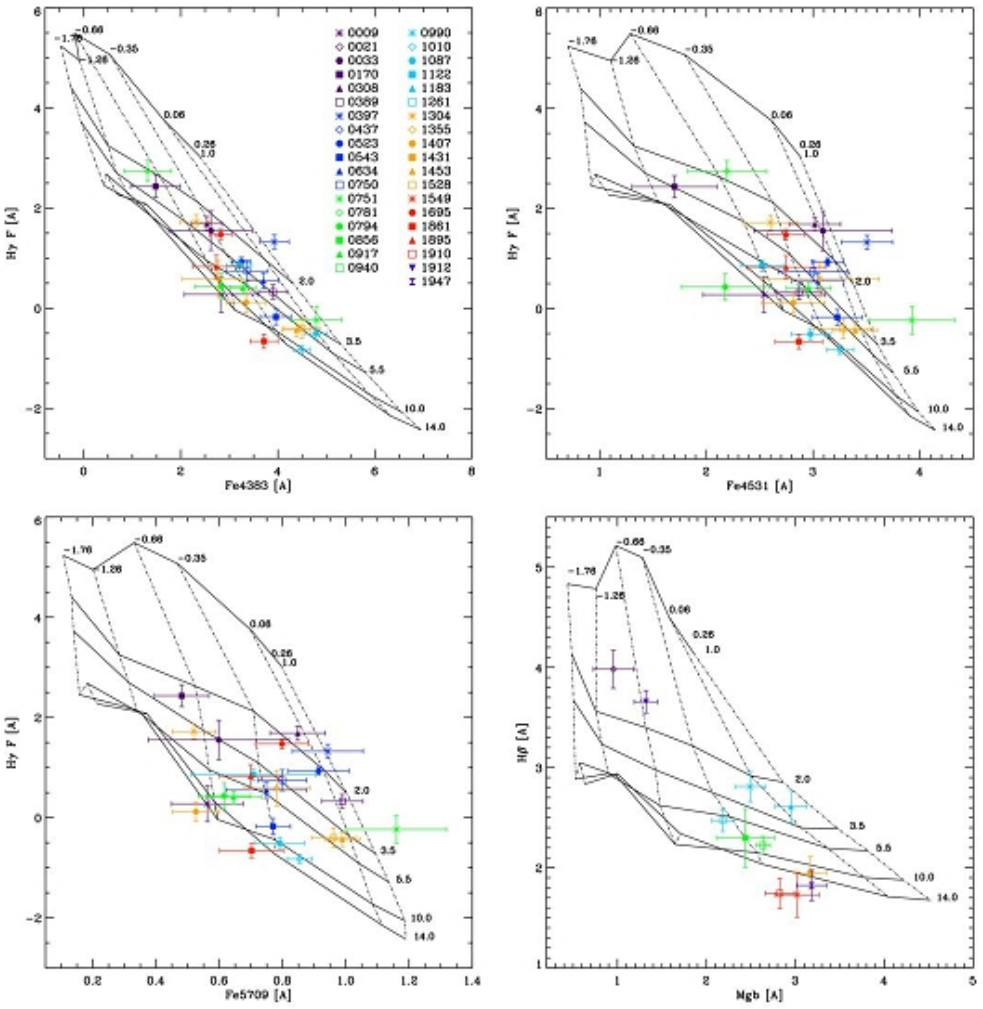

Figure 1. Spectral index-index diagrams used to estimate the stellar populations using solar-scaled theoretical isochrone grids with IMF slope of 1.3 from Vazdekis et al. (2010) in the system LIS-5 Å, solid lines indicate constant age 1.0, 2.0, 3.5, 5.5, 10.0 and 14.0 Gyr, respectively while dotted lines indicate constant [M/H] -1.76, -1.26, -0.65, -0.35, +0.06 and +0.26, respectively.

А вот кальций и натрий никакого доверия не вызывают…(

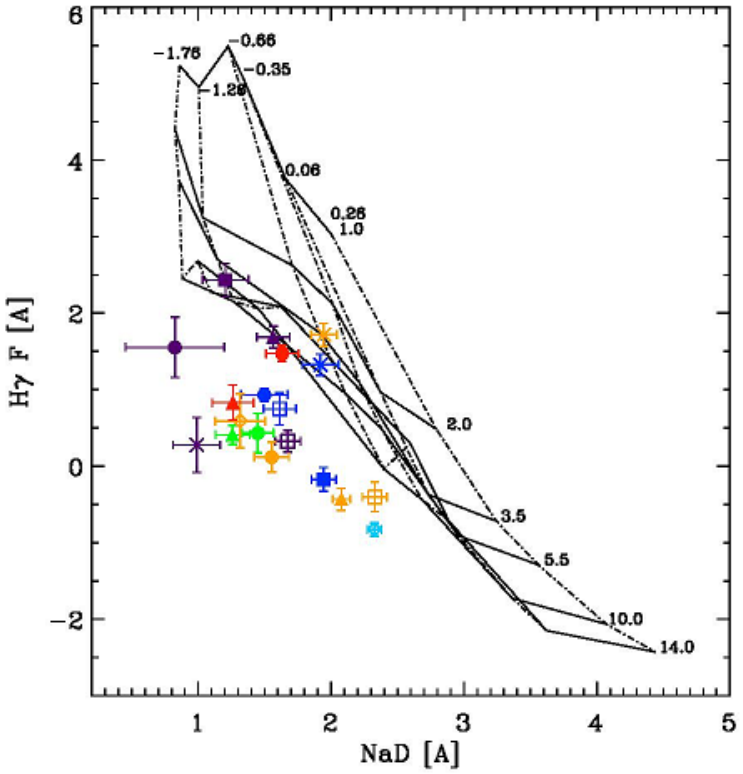

Figure 2. Example of a spectral index-index diagram for $H\gamma_F$ versus NaD, showing that the NaD values are much lower than the predicted by models. Models from Vazdekis et al. 2010. Constant age and [M/H] as in Figure 1.

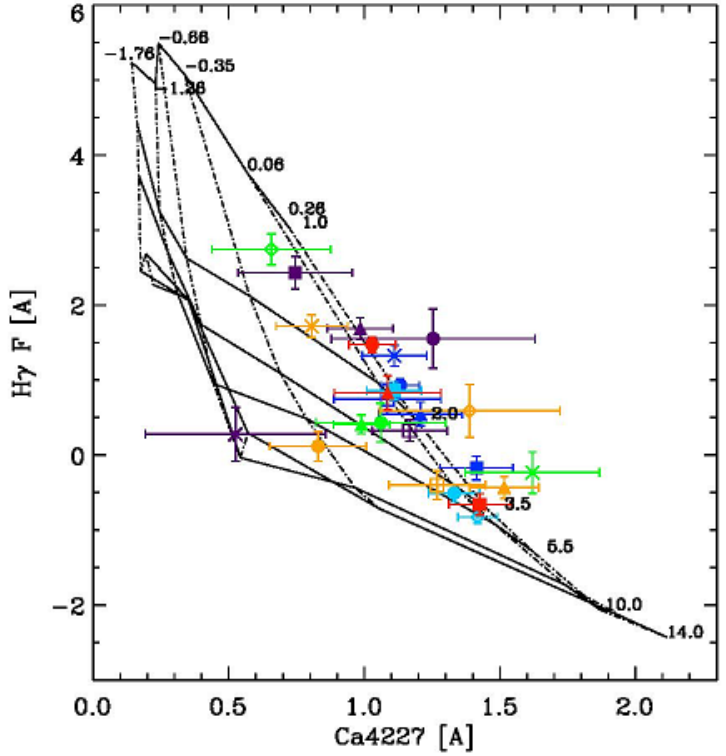

Figure 3. Example of spectral index-index diagram for $H\gamma_F$ versus Ca4227, showing that the Ca4227 values are slightly higher than predicted by models. Models from Vazdekis et al. 2010. Constant age and [M/H] as in Figure 1.

Интерпретация тоже не вызывала бы доверия, если бы не была традиционной

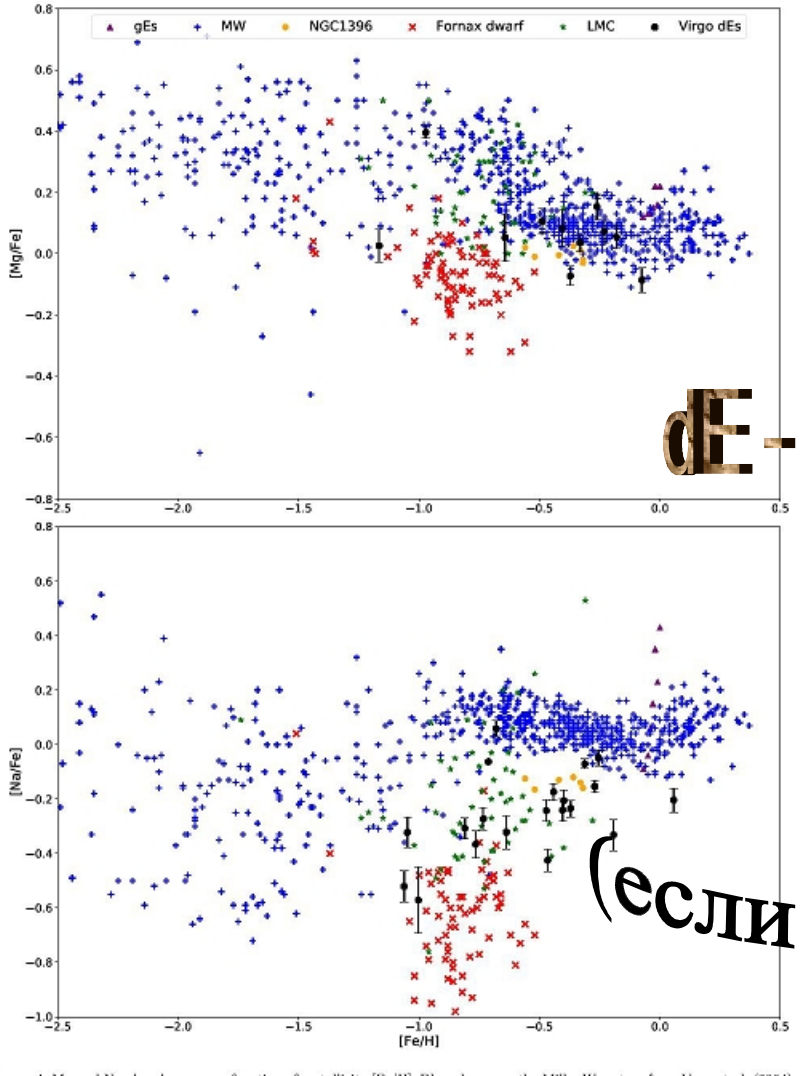

dE - остатки ободранных спиралей

(если не обращать внимание на их натрий).